
Article:
Zhang, K, Bai, L, Lin, G et al. (2 more authors) (2019) Experimental study on pool boiling in a porous artery structure. Applied Thermal Engineering, 149. pp. 377-384. ISSN 1359-4311

https://doi.org/10.1016/j.applthermaleng.2018.12.089

Experimental study on pool boiling in a porous artery structure

Kai Zhang[a], Lizhan Bai[a,*], Guiping Lin[a], Haichuan Jin[a], Dongsheng Wen[a,b,*]

[a]Laboratory of Fundamental Science on Ergonomics and Environmental Control, School of Aeronautic Science and Engineering, Beihang University, Beijing 100191, PR China

[b]School of Chemical and Process Engineering, University of Leeds, Leeds, LS2 9JT, UK

Abstract: In this work, a porous artery structure is proposed to enhance the critical heat flux (CHF) of pool boiling based on the concept of "phase separation and modulation", and extensive experimental studies have been carried out for validation. In the experiment, multiple rectangular arteries were machined directly into the top surface of a copper rod to provide individual flow paths for vapor escaping. The arteries were covered by a microporous copper plate where capillary forces can be developed at the liquid/vapor interface to prevent the vapor from penetrating the porous structure and realize strong liquid suction simultaneously. The pool wall was made of transparent quartz glass to enable a visualization study where the liquid/vapor distribution and movement can be observed directly. Favorable results have been reached as expected, and a maximum heat flux up to 805 W/cm^2 was achieved with no indication of any dry-out, which successfully validated this new concept. In addition, the effects of the diameter and thickness of the porous copper plate, and the connection method between the porous copper plate and copper fin on the pool boiling heat transfer in the porous artery structure were investigated, and the inherent physical mechanisms were analyzed and discussed.

Keywords: pool boiling; critical heat flux; porous structure; experiment

* Corresponding authors. Tel.: +86 10 8233 8600; Fax: +86 10 8233 8600
E-mail address: bailizhan@buaa.edu.cn (L. Bai)

1 Introduction

As a highly efficient way of heat transfer, pool boiling proceeds in the form of latent heat during the liquid/vapor phase change, which can transport a large amount of heat with relatively small temperature difference between the heated surface and the bulk fluid. So far, pool boiling plays an important role in a wide range of applications from large scale electricity power generation, energy storage, desalination systems and refrigeration and air conditioning units to compact small scale systems such as electronics cooling, sterilization and clearing [1-3].

Although pool boiling is a very efficient heat transfer mode, the critical heat flux (CHF) becomes a main limiting factor for pool boiling on a plain surface, beyond which the temperature of the heated surface will rise suddenly, leading to severe deterioration in the heat transfer performance. As the heat flux increases, more and more bubbles are generated at the heated surface, which coalesce to form "bubble mushrooms" and prevent the liquid from rewetting the heated surface. The consequence is that a thin vapor film completely enveloping the hot-spot establishes a thermal barrier between the heated surface and the bulk fluid, which is also termed as boiling crisis [4]. A low CHF is not desirable in practical engineering applications as it would lead to the failure of nucleate boiling and the resultant very rapid burn-out of relevant devices to be cooled, which should be strictly avoided.

Recently for some particular applications especially in some cutting-edge technical fields such as the high power solid laser, advanced miniaturized high-power electronics, advanced nuclear power reactors, highly concentrated photovoltaic and re-entry of hypersonic vehicle, the heat flux generated in these systems has reached several hundred Watts per square centimeter, and still keeps an ever-growing trend. The heat flux to be dissipated is far beyond the CHF of nucleate boiling for

a conventional working fluid on a plain surface, and the cooling issue has undoubtedly become a bottleneck restricting the further development of these promising technologies. It is quite urgent and of great importance to substantially enhance the CHF of nucleate boiling, which has long been a research hotspot in the area of heat transfer and attracts the interest of quite a lot of researchers worldwide.

Extensive theoretical and experimental research has been conducted to enhance the pool boiling CHF. Different theoretical models on the CHF of pool boiling have been developed [5-9], and most models were derived from the hydrodynamic instability model proposed by Zuber et al. [5] and Dhir et al. [6]. They hypothesized that when the velocity of escaping vapor columns reached a threshold value, the interface wave of vapor columns would be affected by the Rayleigh-Taylor instability and Kelvin-Helmholtz instability resulting from the interaction between neighboring vapor columns. Some researchers devoted to revising the hydrodynamic instability model because this model neglected the effect of the bottom heating surface. Based on the hydrodynamic instability model, recent studies regarding the effects of the heating surface characteristics made some modifications considering the surface wettability [10-15], contact angle[16-18], and capillary wicking [19-20]. In order to study these parameters, some optimization measures were presented, such as using surface coating [21-28] to change the surface wettability and contact angle, adopting porous structures [29-33] to enhance the capillary force and utilizing nano/micro grooved surfaces [34-45] to change the morphology of the heated surface.

In particular, the employment of porous structure focused on controlling the hydrodynamic instability wavelength by changing the characteristic length of porous structure in micro and millimeter scales [32]. It was found that the hydrodynamic instability wavelength was related to a

variety of factors such as the pore size, surface pore distribution, the pitch of porous cones, surface tension of liquid, and densities of liquid and vapor, etc. All of the above optimization methods can realize a larger CHF compared to pool boiling on a smooth surface in varying degrees. For instance, Hwang et al. [23] experimentally examined the pool boiling on thin uniform porous coatings using different copper particle diameters (between 40 and 80 μm), fabrications (loosely packed, shaken, or pressed), and particle characteristics (solid or porous particle) with coating thickness varying between 3 and 5 particle diameters. Experimental results showed that the CHF was enhanced to about 1.8 times for all the coatings compared with that on a plain surface. Li et al. [46-47] conducted an experimental investigation of the pool boiling CHF and heat transfer coefficient (HTC) using several kinds of uniform and modulated porous structures made of sintered copper particles. The modulated porous structure reached a CHF of 450 W/cm^2, which was about 3 times of that on a plain surface.

However, for the current porous structures applied in pool boiling enhancement, the existence of liquid/vapor counter flow still limits the CHF to a large extent. With the increase of heat flux, the escaping bubble will impede the replenishment of the liquid to the heated surface, causing insufficient liquid supply and the occurrence of CHF. In order to avoid or mitigate the adverse influence of liquid/vapor counter flow, novel porous structures should be adopted to realize further enhancement of the CHF of pool boiling.

According to the analysis above, a novel porous artery structure is proposed in this work based on the concept of “phase separation and modulation”, aiming to further increase the CHF of pool boiling. Owing to the capillary pressure developed in the porous structure adjacent to the heated surface, this novel structure can actively formulate the flow paths for liquid replenishment to the

heated surface and vapor escaping from the heated surface, with considerably reduced liquid/vapor counter flow. Extensive experimental studies have been conducted to validate this new concept, and desirable results have been achieved. The maximum heat flux up to 805 W/cm^2 has been achieved, which is only limited by the design temperature of the copper heater. In addition, the effects of some relevant parameters on the pool boiling heat transfer in the porous artery structure are also investigated, and the inherent physical mechanisms are analyzed and discussed.

2 Experimental system and data reduction

2.1 Experimental setup

Figure 1 shows schematically the experimental system in this study, which is composed of a visual camera system, a transparent boiling pool, a copper rod with the porous artery structure, a high frequency electromagnetic heater, and a temperature measurement and data acquisition system. The wall of the boiling pool was made of quartz glass with an inner diameter of 200 mm and height of 150 mm to enable a visualization study, and the bottom plate was made of stainless steel with a thickness of 1.0 mm to support the glass wall. There was a through hole located at the center of the bottom plate to allow the copper rod to pass through and heat the working fluid directly. The small gap between the copper rod and the bottom plate was filled with mixed silicone mainly for sealing purpose, which can also effectively reduce the thermal conduction from the copper rod to the bottom plate. Water was selected as the working fluid, and the boiling pool was directly open to the ambient, under which condition the working fluid should be always under the standard atmospheric pressure with a constant saturation temperature of 100 ℃. A high frequency electromagnetic heater was employed to provide very high heat flux, whose output power can be continuously adjusted within the range of 0-15 kW.

In the experiment, the upper and lower parts of the copper rod were an entity, and the upper part was not interchangeable. The lower part of the copper rod had a constant diameter of 20 mm and a constant height of 35 mm, while the upper part had a constant height of 16 mm. There were four test samples each with a different upper-part diameter, to match the varying diameter of the microporous copper plate. There were totally three holes with a depth of 2 mm in the side surface of the upper part of the copper rod, where three type K thermocouples were fixed tightly, as shown in Fig. 2. Figure 2 shows the porous artery structure proposed in this work, where multiple rectangular arteries were machined directly in the top surface of the copper rod, and a micro-porous copper plate was sintered directly on the top surface of the fins with a high temperature of about 900℃ for one hour. Fig. 3 shows the SEM photo of the microporous copper plate, in which the mesh count of the porous plate is 30-40, corresponding to the particle diameter range of 380-550μm . The temperature measurement and data acquisition system were composed of three type K thermocouples and an Agilent 34970A Data Acquisition System, which was used to monitor the temperature change at an interval of 2 s. The Agilent 34970A was linked to a computer for data display and storage. Table 1 shows the basic parameters of the porous artery structure.

2.2 Data reduction and uncertainty analysis

At a steady state, the temperature gradient in the axial direction of the copper rod ($\mathrm{d}T/\mathrm{d}s$), heat flux (q), superheat (ΔT) and the boiling heat transfer coefficient (h) can be calculated through the following equations, respectively.

The temperature gradient was estimated using Taylor's backward series approximation:

$$\frac{\mathrm{d}T}{\mathrm{d}s} = \frac{3T_{\mathrm{TC1}} - 4T_{\mathrm{TC2}} + T_{\mathrm{TC3}}}{2s_1} \tag{1}$$

where T_{TC1}, T_{TC2}, T_{TC3} represent the temperature data obtained from the three thermocouples, respectively, and s_1 is the distance between the measurement points TC1 and TC2.

The heat flux at the heated surface was calculated using the Fourier's law of heat conduction:

$$q = -\lambda \frac{\mathrm{d}T}{\mathrm{d}s} \tag{2}$$

where λ is the thermal conductivity of copper.

Once the heat flux was acquired, the superheat and heat transfer coefficient can be calculated as follows:

$$\Delta T=T_w\text{-}T_s=T_{TC1}\text{-}\frac{qs_0}{\lambda}\text{-}T_s \tag{3}$$

$$h=\frac{q}{\Delta T} \tag{4}$$

where T_w is the temperature of the heated surface, and T_s is the saturation temperature of water at one atmospheric pressure.

Individual standard uncertainties were considered to estimate the standard deviation of the results, which were calculated using a standard approach as follows:

$$\Delta_q=\sqrt{2\Delta_T^2\left(\frac{\lambda}{2s}\right)^2+\Delta_s^2\left[\frac{\lambda(T_{TC3}\text{-}T_{TC1})}{2s^2}\right]^2} \tag{5}$$

$$\Delta_{\Delta T}=\sqrt{\Delta_T^2+\frac{q^2}{\lambda^2}\Delta_s^2+\frac{s_0^2}{\lambda^2}\Delta_q^2} \tag{6}$$

$$\Delta_h=\sqrt{\frac{q^2}{(\Delta T)^4}\Delta_{\Delta T}^2+\frac{\Delta_q^2}{(\Delta T)^2}} \tag{7}$$

The uncertainty of the temperature measurement (Δ_T) through the thermocouples was about ± 0.5 °C, and the uncertainty of the distance between adjacent thermocouple locations (Δ_s) was approximately ± 0.20 mm. The relative uncertainty of the heat flux was found less than 3.0% when the heat flux was larger than 100 W/cm^2. The maximum uncertainty for the heat transfer coefficient was calculated to be less than 5.0% in all cases. The copper rod was enveloped by high temperature thermal insulation materials (asbestos fiber) with a thickness larger than 6.0 cm, whose thermal conductivity is below 0.1 W/ (m K), to reduce the heat loss from the surface of the copper rod to the ambient surroundings. The total heat loss from the copper rod to the environment was estimated to be within 4.0%.

3 Experimental results and discussions

3.1 Temperature data and visualization study

Figure 4 shows the temperature changes of the three thermocouples attached on the upper part of the copper rod in an experimental test, and Fig. 5 shows the liquid/vapor distribution and movement for pool boiling in the porous artery structure with different heat fluxes. In Figs. 4 and 5, the diameter of the upper part of the copper rod was 8 mm, and the thickness of the porous copper plate was 2.0 mm.

In Fig. 4, the power output of the electromagnetic heater was first set at a fixed value, and when the thermocouple temperatures became stable for a while, i.e., about 5 minutes, the power output was adjusted to a higher level. The heat flux in Fig. 4 was calculated based on equation (1) when the three thermocouples (TC1, TC2 and TC3) reached a stable state. As shown in Fig. 4, with the increase of the power output of the electromagnetic heater, the temperature differences between TC1 and TC2 and between TC2 and TC3 both became larger accordingly, indicating a larger heat flux along the axial direction of the copper rod according to equation (2). When the heat flux was below 529 W/cm^2, the temperatures of the three thermocouples could reach a steady state quickly; however, when the heat flux was further increased to a value a little larger than 529 W/cm^2, the thermocouple temperatures rose very sharply, indicating that boiling crisis should occur. Under this condition, the electromagnetic heater must be switched off immediately; otherwise the heater would be burnt out.

From Fig. 5 (a) and (b), it can be clearly observed that with relatively small heat fluxes, i.e., 188 and 236 W/cm^2, the bubbles generated at the heated surface escaped from the two ends of the arteries without mutual interaction and impact. Under this condition, the liquid replenishment to the heated surface was mainly from the top surface of the microporous structure, while the vapor venting from the heated surface was through the multiple arteries to the boiling pool, which successfully validated the concept of "phase separation and modulation".

At moderate heat fluxes, i.e., 338 and 482 W/cm^2 in Figs.5 (c) and (d), more and more vapor was generated at the heated surface, and a relatively large vapor column existed at each end of the arteries. Although the two vapor columns swung violently at two sides of the porous plate, they did not interact with each other. Under this condition, it was still easy to achieve liquid supply to the heated surface and vapor venting from the heated surface in this porous artery structure. However, at large

heat fluxes, i.e., 529 W/cm^2 in Fig.5 (e), because so much vapor was generated at the heated surface that the two vapor columns at the two sides of the porous plate coalesced, and a mushroom-like vapor slug was located over the porous copper plate, which would adversely affect the liquid supply from the top surface of the porous structure to some extent. When the heat flux was further increased to an even higher value, the generated vapor would envelop the whole porous copper plate, and under which condition the liquid replenishment to the heated surface would be completely impossible, corresponding to the occurrence of the CHF, as shown in Fig.5 (f). Because the heat generated in the copper rod was difficult to be transferred to the working fluid, the thermocouple temperatures rose very sharply, as shown in Fig. 4, which would cause serious accident in practical applications.

3.2 Comparison with different cases

Figure 6 shows the superheat dependence of the heat flux for pool boiling with different cases being as 1) a plain surface, 2) a surface with only rectangular channels and 3) a surface with both rectangular arteries and a microporous layer, together with a well-known nucleate boiling correlation, i.e., the Rohsenow correlation. In Fig. 6, the width and depth of the rectangular channel were 0.8 and 1.5 mm respectively; and the thickness and diameter of the microporous copper plate were 4.0 and 8.0 mm respectively. In the Rohsenow correlation, the fluid-surface constant C_{sf} was set as 0.0128 for the combination of water on polished copper, as suggested by Vachon, Nix and Tangor.

According to Fig. 6, the pool boiling heat transfer performance on a plain surface predicted by the Rohsenow correlation is obviously better than the experimental results in this work when the superheat is relatively large, i.e., greater than 15.0 ℃, that is mainly because C_{sf} is an empirical value, and it is very difficult to determine an accurate value fully accounting for the micromorphology of the heating surface. For the pool boiling on a plain surface with only rectangular channels, the heat transfer performance is much better than that on a plain surface, due to obviously extended heat transfer area and the slight capillary action developed in the channels. While for the porous artery structure, it possesses the best pool boiling heat transfer performance, which can achieve a significantly enhanced CHF, several times of that on a plain surface, as evidenced by the experimental results.

Repeatability test is really important in the experimental study of pool boiling. In fact, the authors have conducted multiple tests for pool boiling in the porous artery structure with specific structural parameters. It is found that the repeatability is not good for this experimental system. The pool boiling performance in the porous artery structure for the first test was the best; however, it became worse and worse with subsequent repeatability tests. The authors think the pool boiling performance degradation is mainly caused by the oxidation action of the microporous copper plate, because the experiment is conducted in an open environment where oxygen dissolved in the water will inevitably react chemically with the copper particle. A direct evidence is that the microporous copper plate gradually changed from the initial yellow color to black as the repeatability tests proceeded. When copper oxide is produced at the outer surface of the copper particle, it will pose an adverse effect on the pool boiling heat transfer performance: on one hand, its thermal conductivity is far smaller than that of pure copper, leading to increased thermal resistance in heat conduction; one the other hand, it will reduce the pore size of the porous plate and result in increased flow resistance.

3.3 Effect of the diameter of porous plate

Figure 7 shows the superheat dependence of the heat flux with different diameters of the copper porous plate. In Fig. 7, the thickness of the porous plate was kept at 2mm, and the diameter of the porous plate was selected as 6, 8, 10 and 12 mm in sequence.

In Fig. 7, for the porous artery structure with fixed diameter and thickness of the porous plate, the superheat dependence of the heat flux exhibited very similar trends: the heat flux first increased quickly with the increase of the superheat, and after reaching a certain value, it began to increase much slowly, corresponding to much reduced boiling heat transfer performance. This phenomenon should be attributed to imperfect contact between the copper porous plate and the fins at the top surface of the copper rod, as schematically shown in Fig. 8. Because the surface of the copper porous plate cannot be absolutely flat, there existed several sub-millimeter scale gaps between the copper porous plate and the copper fin, although they were sintered together here. At small and moderate heat fluxes, the vapor velocity in the arteries was relatively small, and the pressure drop of the vapor flow in the arteries was not large accordingly. Under this condition, liquid/vapor two phase working fluid can still exist in the gaps between the copper porous plate and the fins of the copper rod, and the capillary pressure developed at the liquid/vapor interface was enough to drive the vapor to flow

out of the arteries.

However, with further increase of the heat flux, more and more vapor was generated, resulting in increased vapor velocity and pressure drop in the arteries. Under such a condition, the small capillary pressure developed in the gaps between the copper porous plate and the copper fins would become insufficient to drive the vapor flow, and the liquid in the gaps receded into the copper porous plate, where much larger capillary pressure can be developed at the liquid/vapor interface to drive the vapor flow. Because the gaps were totally occupied by the vapor, whose thermal conductivity is very small, the heat transfer from the copper fins to the liquid/vapor interface within the copper porous plate was mainly through the conduction of the copper particles directly contacting the copper fins, leading to additional thermal resistance and much reduced heat transfer performance, as evidenced in Fig. 7.

Someone may ascribe the change in the boiling curve slope to the transition from nucleate boiling regime to the transitional boiling regime instead of the bad contact analyzed above. The authors do not agree with this viewpoint, based on the following two reasons. First, according to the classic pool boiling theory, in the transitional boiling regime, the heat flux decreases with increasing superheated degree. However, in our experiments, the heat flux always increases with increasing superheated degree, although the boiling curve slope obviously becomes smaller after the turning point at high heat fluxes. Second, at very high heat fluxes after the turning point, the liquid and vapor flow paths in the porous artery structure are still normal as expected, i.e., the liquid is replenished from the top surface of the microporous copper plate to the liquid/vapor interface, and vapor generated in the microporous structure escapes from the vapor channels to the boiling pool. No any indication for the transitional boiling regime can be observed.

Figure 7 shows that larger diameter of the copper porous plate leads to lower pool boiling heat transfer performance under the same superheat, especially when the superheat is larger than 30 ℃. For instance, when the diameter of the copper porous plate was 6, 8, 10 and 12 mm, the heat flux could reach 523, 398, 263 and 208 W/cm^2 in sequence with the same superheat of 50 ℃, which exhibited an obvious decreasing trend. In addition, the smaller the diameter of the copper porous plate, the larger the heat flux at the turning point of the curve in Fig. 7. The experimental results seemed reasonable. As the maximum artery length was equal to the diameter of the copper porous

plate, larger diameter of the copper porous plate will cause an increase of the vapor flow resistance in the arteries, and the vapor front will recede within the copper porous plate, resulting in increased conduction thermal resistance and reduced boiling heat transfer performance. It should be of note that the last data point on each curve in Fig. 7 does not correspond to the data point just before the CHF. In most cases, the experiments were terminated for safety consideration because the temperature at the bottom part of the copper rod became rather high, sometimes nearly approaching 800 ℃. To reach the true CHF for the porous artery structure, improved heater design is still needed.

3.4 Effect of the thickness of porous plate

Figure 9 shows the superheat dependence of the heat flux with different thicknesses of the copper porous plate. In Fig. 9, the diameter of the porous plate was kept at 8 mm, and the thickness of the porous plate was selected as 2, 3 and 4 mm in sequence.

Figure 9 clearly shows that with the increase of the thickness of the copper porous plate, significant improvement in the pool boiling CHF can be achieved. In Fig. 9, when the thickness of the porous plate was 3mm and 4mm, the maximum heat flux reached 780 and 806 W/cm^2 respectively. However, these values did not reach the CHF, which was only limited by the maximum allowable temperature of the copper heater. For security reason, the maximum temperature of the copper rod was limited by 800 °C in all the experiments. So in the experiments with the porous plate thickness of 3 mm and 4 mm, we did not observe the occurrence of the CHF, i.e., the porous plate was totally enveloped by vapor, as shown in Fig.5 (f) above. This result well agreed with the experimental data from Li, et al. [25-26], where copper wire mesh with uniform thickness was utilized to enhance the CHF of pool boiling, and the CHF was found to increase initially with increasing porous coating thickness when the volumetric porosity and mesh size were held constant. The cause for CHF increases with increasing thickness of conductive porous coatings was believed to be the augmentation of the effective heat transfer area, and the reduction in the flow resistance in the horizontal direction because of the increase of the flow area for the liquid phase. It should be of note that for the boiling heat transfer tests with different diameters, i.e., 6, 10 and 12 mm, the boiling curves showed very similar trends to that shown in Fig. 9.

So far, using microporous surfaces to enhance the pool boiling CHF has become an attractive

method, and several similar methods have already been reported. At the same time, different theories for the CHF of microporous surfaces have been suggested, including the viscous-capillary model, hydrodynamic instability model, and the dry-out of the porous coatings, etc. In general, all these theories account for some aspects of the pool boiling phenomena. The hydrodynamic instability model is mainly responsible for the bulk liquid/vapor two-phase fluid above the heated surface, i.e., independent of the thickness of the microporous coatings; while the viscous-capillary model and the dry-out of the porous coatings are mainly responsible for the heated surface. Therefore, a perfect unified theory currently is still not available, and a comprehensive understanding on the CHF mechanism for the microporous surfaces is crucial.

Li, et al. [25-26] adopted a uniform thickness porous structure to enhance the pool boiling CHF, and the maximum value a little larger than 350 W/cm^2 was achieved with an optimum thickness of the porous structure. The enhancement mechanism is mainly the reduction in the heat flux density on the heated wall due to the fin effect and the improved liquid supply resulting from the capillary induced flow. For the porous structure with a uniform thickness, the thickness should be smaller than the bubble departure diameter; otherwise it will impede the vapor escape, causing reduced pool boiling heat transfer performance and reduction in the CHF. Li, et al. [46-47] employed a modulated porous structure to enhance the pool boiling heat transfer, and a maximum CHF of about 450 W/cm^2 was achieved. In order to reduce the large surface superheat (>100) for pool boiling at very high heat fluxes, some innovative work has been carried out by Ha and Graham [48] where multiple channels were fabricated into the microporous structure to allow vapor escape. An obvious enhancement in the CHF and heat transfer coefficient was achieved, allowing CHF greater than 350 W/cm^2 at a superheat less than 50 °C. For the researches by Li, et al. [46-47] and Graham [48], the enhancement mechanism is mainly the modulation of liquid/vapor pathway to delay the Rayleigh-Taylor instability, besides the extended heat transfer area and improved liquid supply. In this work, an even higher pool boiling CHF in the porous artery structure was acquired, that was mainly because it can modulate the liquid/vapor pathway with a much stronger capability due to this innovative structure design.

3.5 Effect of connection method between porous plate and copper fin

Here, we also compared the effect of the connection method between the copper porous plate and

the copper fin on the pool boiling performance, where the diameters of the porous plate were selected as 8mm and 10mm respectively. Two connection methods have been tested: one type of the connection was by silver brazing, and the other is by sintering at a temperature of 900 ℃ for one hour. The two different connection methods affected the pool boiling heat transfer performance significantly, as shown in Fig. 10.

In Fig. 10, when the copper porous plate was connected to the copper fin by silver brazing, the heat flux always increased quickly with increasing superheat, and no obvious deterioration in the boiling heat transfer performance occurred; however, when the copper porous plate was connected to the copper fin by the sintering method, an obvious turning point on the heat flux curve could be observed at relatively large superheat, and significant deterioration in the boiling heat transfer performance was observed at high heat fluxes. As illustrated in Fig. 8, the deterioration in the pool boiling heat transfer performance should be caused by imperfect contact between the copper porous plate and the copper fin when the sintering method was adopted. When silver brazing was used instead, as most of the sub-millimeter scale gaps between the copper porous plate and the copper fin can be filled by highly conductive brazing filler metals, whose thermal conductivity is far larger than that of pure vapor, very good thermal contact performance can be guaranteed even at very large heat fluxes. Under this condition, no obvious deterioration in the pool boiling heat transfer performance will occur in all the heat flux range, as shown in Fig. 10.

4 Conclusions

Based on the concept of "phase separation and modulation", a porous artery structure was proposed to enhance the CHF of pool boiling, and extensive experimental studies have been carried out in this work. According to the experimental results and theoretical analysis, some important conclusions have been drawn, as summarized below:

- The porous artery structure proposed here can effectively realize the liquid/vapor phase separation in the pool boiling: liquid supply is mainly from the top surface of the copper microporous structure, while vapor venting from the liquid/vapor interface is through the multiple arteries to the boiling pool, enabled by the capillary pressure developed within the porous structure. As a result, rather high heat flux, i.e., 806 W/cm^2, has been achieved with no occurrence of the dry-out phenomenon, due to considerably reduced liquid/vapor counter flow.

- The pool boiling heat transfer performance decreases with increasing diameter of the copper porous plate, especially at relatively large heat fluxes, which is mainly caused by increased vapor flow resistance in the arteries.
- The pool boiling heat transfer performance increases with increasing thickness of the copper porous plate, especially at relatively large heat fluxes, which is believed to be due to augmentation of the effective heat transfer area, and the reduction in the liquid flow resistance in the horizontal direction because of the increase of the flow area.
- The connection method between the porous plate and the copper fin significantly affects the pool boiling heat transfer performance. At large heat fluxes, severe deterioration occurs in the pool boiling heat transfer performance when the sintering method is adopted, due to imperfect contact between the porous plate and the copper fin. Using silver brazing instead is a good solution, as the gaps between the porous plate and the copper fin can be filled by highly conductive brazing filler metals.

Acknowledgements

This work was supported by the National Natural Science Foundation of China (No. 51776012) and Beijing Natural Science Foundation (No.3182023).

References

[1] V.P. Carey, Liquid Vapor Phase Change Phenomena: An Introduction to the Thermophysics of Vaporization and Condensation Processes in Heat Transfer Equipment, 2nd ed. Taylor & Francis, 2007

[2] Arvind Jaikumar, Satish G. Kandlikar, Enhanced pool boiling for electronics cooling using porous fin tops on open microchannels with FC-87, Applied Thermal Engineering 91(2015) 426-433

[3] Steven B. White, Albert J. Shih, Kevin P. Pipe, Effects of nanoparticle layering on nanofluid and base fluid pool boiling heat transfer from a horizontal surface under atmospheric pressure, Journal of Applied Physics 107(2010) 1-6

[4] A. Zou, Shalabh C. Maroo, Critical height of micro/nano structures for pool boiling heat transfer enhancement, Applied Physics Letters 103(2013), paper No. 221602

[5] N. Zuber, On the stability of boiling heat transfer, Trans. Am. Soc. Mech. Eng. 80 (2) (1958) 457–466.

[6] V.K. Dhir, J.H. Lienhard, Hydrodynamic prediction of peak pool-boiling heat fluxes from finite bodies, J. Heat Transf. 95 (2) (1973) 152-158.

[7] R.F. Gaertner, Photographic study of nucleate pool boiling on a horizontal surface, J. Heat Transf. 8 (1) (1965) 17-27.

[8] R. Webb, Nucleate boiling on porous coated surfaces, Heat Transf. Eng. 4 (3-4) (1981) 71-82.

[9] V.K. Dhir, Framework for a unified model for nucleate and transition pool boiling, J. Heat Transf. 111 (3) (1989) 739-746.

[10] S.J. Kim, I.C. Bang, J. Buongiorno, L. Hu. Surface wettability change during pool boiling of nanofluids and its effect on critical heat flux, Int. J. Heat Mass Transf. 50 (19–20) (2007) 4105-4116.

[11] K.H. Chu, R. Enright, E. Wang, Structured surfaces for enhanced pool boiling heat transfer, Appl. Phy. Lett. 100 (24) (2012), paper No. 241603.

[12] M.M. Rahman, E. Ölçeroğlu, M. Mccarthy, Role of wickability on the critical heat flux of structured superhydrophilic surfaces, Langmuir 30 (37) (2014) 11225–11234.

[13] T.P. Hai, N. Caney, P. Marty, S. Colasson, J. Gavillet, Surface wettability control by nanocoating: The effects on pool boiling heat transfer and nucleation mechanism, Int. J. Heat Mass Transf. 52 (23–24) (2009) 5459-5471.

[14] J.S. Lee, J.S. Lee, Critical heat flux enhancement of pool boiling with adaptive fraction control of patterned wettability, Int. J. Heat Mass Transf. 96 (2016) 504-512.

[15] J.S. Lee, J.S. Lee, Numerical approach to the suppression of film boiling on hot-spots by radial control of patterned wettability, Int. J. Multiphase Flow 84 (2016) 165-175.

[16] M. Maracy, R.H.S. Winterton, Hysteresis and contact angle effects in transition pool boiling of water, Int. J. Heat Mass Transf. 31 (7) (1988) 1443-1449.

[17] L. Liao, R. Bao, Z. Liu, Compositive effects of orientation and contact angle on critical heat flux in pool boiling of water, Heat Mass Transf. 44 (12) (2008) 1447-1453.

[18] S.G. Kandlikar, A theoretical model to predict pool boiling CHF incorporating effects of contact angle and orientation, J. Heat Transf. 123 (6) (2001) 1071-1079.

[19] J. Kim, S. Jun, R. Laksnarain, S.M. You, Effect of surface roughness on pool boiling heat transfer at a heated surface having moderate wettability, Int. J. Heat Mass Transf. 101 (2016) 992-1002.

[20] M.M. Rahman, E. Ölçeroğlu, M. Mccarthy, Role of wickability on the critical heat flux of structured superhydrophilic surfaces, Langmuir 30 (37) (2014) 11225–11234.

[21] B. Feng, K. Weaver, G.P. Peterson, Enhancement of critical heat flux in pool boiling using atomic layer deposition of alumina, Appl. Phys. Lett. 100 (5) (2012), paper No. 053120.

[22] S.G. Liter, M. Kaviany, Pool-boiling CHF enhancement by modulated porous-layer coating: theory and experiment, Int. J. Heat Mass Transf. 44 (22) (2001) 4287-4311.

[23] G.S. Hwang, M. Kaviany, Critical heat flux in thin, uniform particle coatings, Int. J. Heat Mass Transf. 49 (5–6) (2006) 844-849.

[24] W. Wu, H. Bostanci, L.C. Chow, Y. Hong, M. Su, Nucleate boiling heat transfer enhancement for water and FC-72 on titanium oxide and silicon oxide surfaces, Int. J. Heat Mass Transf. 53 (9) (2010) 1773-1777.

[25] C. Li, G.P. Peterson, Geometric effects on critical heat flux on horizontal microporous coatings, J. Therm. Heat Transf. 24 (3) (2012) 449-455.

[26] C. Li, G.P. Peterson, Parametric study of pool boiling on horizontal highly conductive microporous coated surfaces, J. Heat Transf. 129 (11) (2007) 1465-1475.

[27] S. Jun, J. Kim, D. Son, H.Y. Kim, S.M. You, Enhancement of pool boiling heat transfer in water using sintered copper microporous coatings, Nucl. Eng. Technol. 48 (4) (2016) 932-940.

[28] M. Dharmendra, S. Suresh, C.S.S. Kumar, Q. Yang, Pool boiling heat transfer enhancement using vertically aligned carbon nanotube coatings on a copper substrate, Appl. Therm. Eng. 99 (2016) 61-71.

[29] C. Li, R.P. Rioux, Independent and collective roles of surface structures at different length scales on pool boiling heat transfer, Sci. Rep. 6 (2016) paper number 37044.

[30] L. Bai, L. Zhang, G. Lin, G.P. Peterson, Pool boiling with high heat flux enabled by a porous artery structure, Appl. Phys. Lett. 108 (23) (2016) 1-6.

[31] L. Bai, L. Zhang, J. Guo, G. Lin, X. Bu, Evaporation/boiling heat transfer characteristics in an artery porous structure, Appl. Therm. Eng. 104 (2016) 587-595.

[32] R.P. Rioux, E.C. Nolan, C. Li, A systematic study of pool boiling heat transfer on structured porous surfaces: From nanoscale through microscale to macroscale, Aip Adv. 4 (11) (2014) 122-141.

[33] C. Li, G.P. Peterson, Evaporation/Boiling in thin capillary wicks (II)—Effects of volumetric porosity and mesh size, J. Heat Transf. 128 (12) (2006) 1320-1328.

[34] A.R. Neto, J.L.G. Oliveira, J.C. Passos, Heat transfer coefficient and critical heat flux during nucleate pool boiling of water in the presence of nanoparticles of alumina, maghemite and CNTs, Appl. Therm. Eng. 111 (2017) 1493–1506.

[35] M. Ray, S. Deb, S. Bhaumik, Pool boiling heat transfer of refrigerant R-134a on TiO2, nano wire arrays surface, Appl. Therm. Eng. 107 (2016) 1294-1303.

[36] D. Zhong, J. Meng, Z. Li, Z. Guo, Experimental study of saturated pool boiling from downward facing surfaces with artificial cavities, Exp. Therm. Fluid Sci. 68 (2015) 442-451.

[37] S. Das, B. Saha, S. Bhaumik, Experimental study of nucleate pool boiling heat transfer of water by surface functionalization with SiO2, nanostructure, Exp. Therm. Fluid Sci. 81 (2017) 454–465.

[38] M.M. Sarafraz, F. Hormozi, S.M. Peyghambarzadeh, Pool boiling heat transfer to aqueous alumina nano-fluids on the plain and concentric circular micro-structured (CCM) surfaces, Exp. Therm. Fluid Sci. 72 (2016) 125-139.

[39] J.Y. Ho, K.K. Wong, K.C. Leong, Saturated pool boiling of FC-72 from enhanced surfaces produced by Selective Laser Melting, Int. J. Heat Mass Transf. 99 (2016) 107-121.

[40] S.H. Kim, G.C. Lee, J.Y. Kang, K. Moriyama, H.S. Park, Heat flux partitioning analysis of pool boiling on micro structured surface using infrared visualization, Int. J. Heat Mass Transf. 102 (2016) 756-765.

[41] H.S. Ahn, L. Chan, J. Kim, M.H. Kim, The effect of capillary wicking action of micro/nano structures on pool boiling critical heat flux, Int. J. Heat Mass Transf. 55 (1) (2012) 89-92.

[42] S. Sinharay, W. Zhang, B. Stoltz, R.P. Sahu, S. Sinharay, Swing-like pool boiling on nano-textured surfaces for microgravity applications related to cooling of high-power microelectronics, Npj Microgravity. 3 (1) (2017) 9-17.

[43] A.H. Seon, K.J. Min, P. Chibeom, J. Ji-Wook, L.J. Sung, A novel role of three dimensional graphene foam to prevent heater failure during boiling, Sci. Rep. 3 (6137) (2013) 1960-1968.

[44] S.P. Malyshenko, Features of heat transfer with boiling on surfaces with porous coatings, Therm. Eng. 38 (2) (1991) 38-45.

[45] C. Ramaswamy, Y. Joshi, W. Nakayama, W.B. Johnson, High-speed visualization of boiling from an enhanced structure, Int. J. Heat Mass Transf. 45 (24) (2002) 4761-4771.

[46] C.H. Li, G.P. Peterson, Experimental study of enhanced nucleate boiling heat transfer on uniform and modulated porous structures, Frontiers in Heat and Mass Transfer 1 (2010) 1-10

[47] C.H. Li, T. Li, P. Hodgins, et al., Comparison study of liquid replenishing impacts on critical heat flux and heat transfer coefficient of nucleate pool boiling on multiscale modulated porous structures, International Journal of Heat and Mass Transfer 54 (2011) 3146-3155

[48] Minseok Ha, and Samuel Graham, Pool boiling characteristics and critical heat flux mechanisms of microporous surfaces and enhancement through structural modification, Appl. Phys. Lett. 111 (2017), No. 091601

Table captions

Table 1 Basic parameters of the porous artery structure

Figure captions

Table 1 Basic parameters of the porous artery structure

Item	Parameter
Diameter of lower part of copper rod (D_1)/mm	20
Diameter of upper part of copper rod (D_2)/mm	6.0, 8.0, 10.0, 12.0
Microporous structure diameter (D_2)/mm	6.0, 8.0, 10.0, 12.0
Microporous structure thickness (H_1)/mm	2.0, 3.0, 4.0
Copper particle diameter range in porous structure/μm	380-550
Artery depth (H_2)/mm	1.5
Distance (s_0, s_1, s_2)/mm	4.0, 4.0, 4.0
Artery width (W_1)/mm	0.8
Fin width (W_2)/mm	0.9

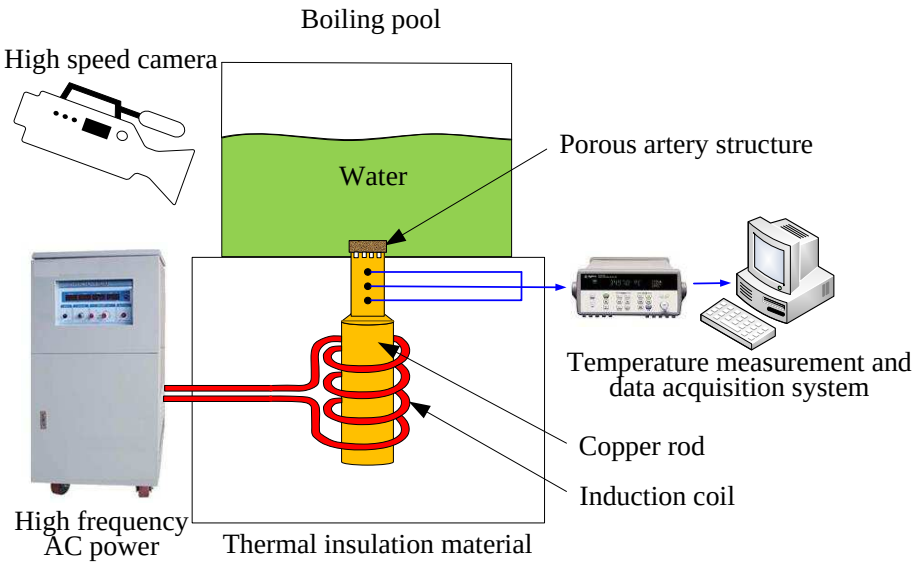

Fig. 1 Schematic of the experimental system

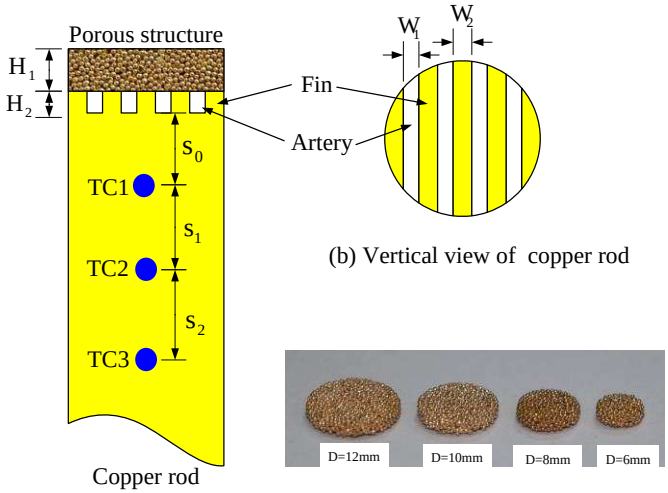

Fig. 2 Schematic of the porous artery structure

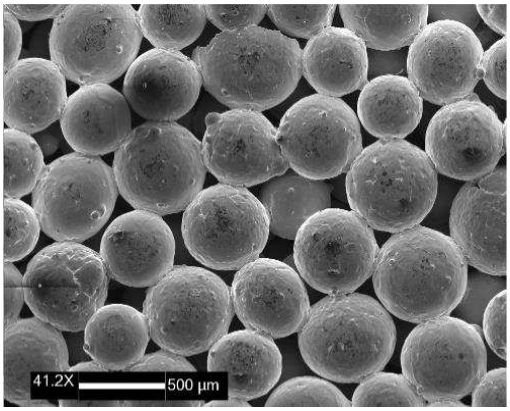

Fig. 3 SEM photo of the microporous copper plate (diameter range 380-550µm)

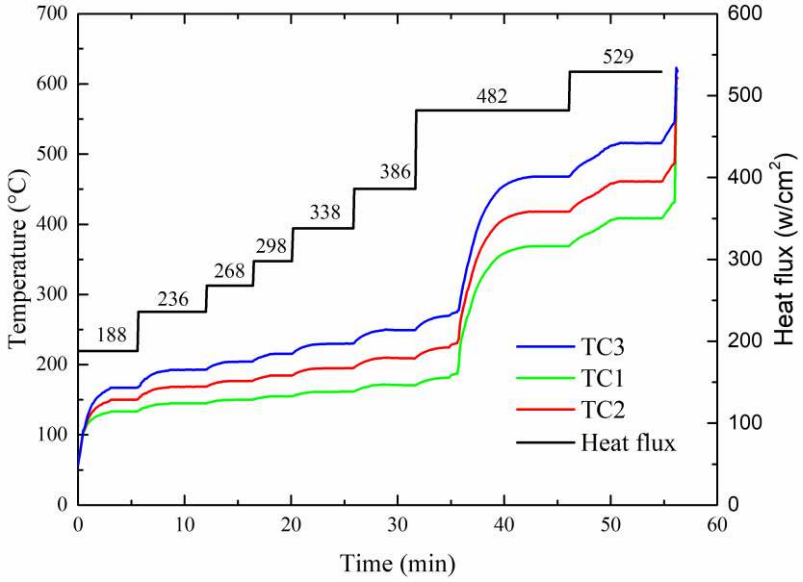

Fig. 4 Temperature changes for different heat fluxes (microporous plate thickness: 2 mm, diameter: 8 mm)

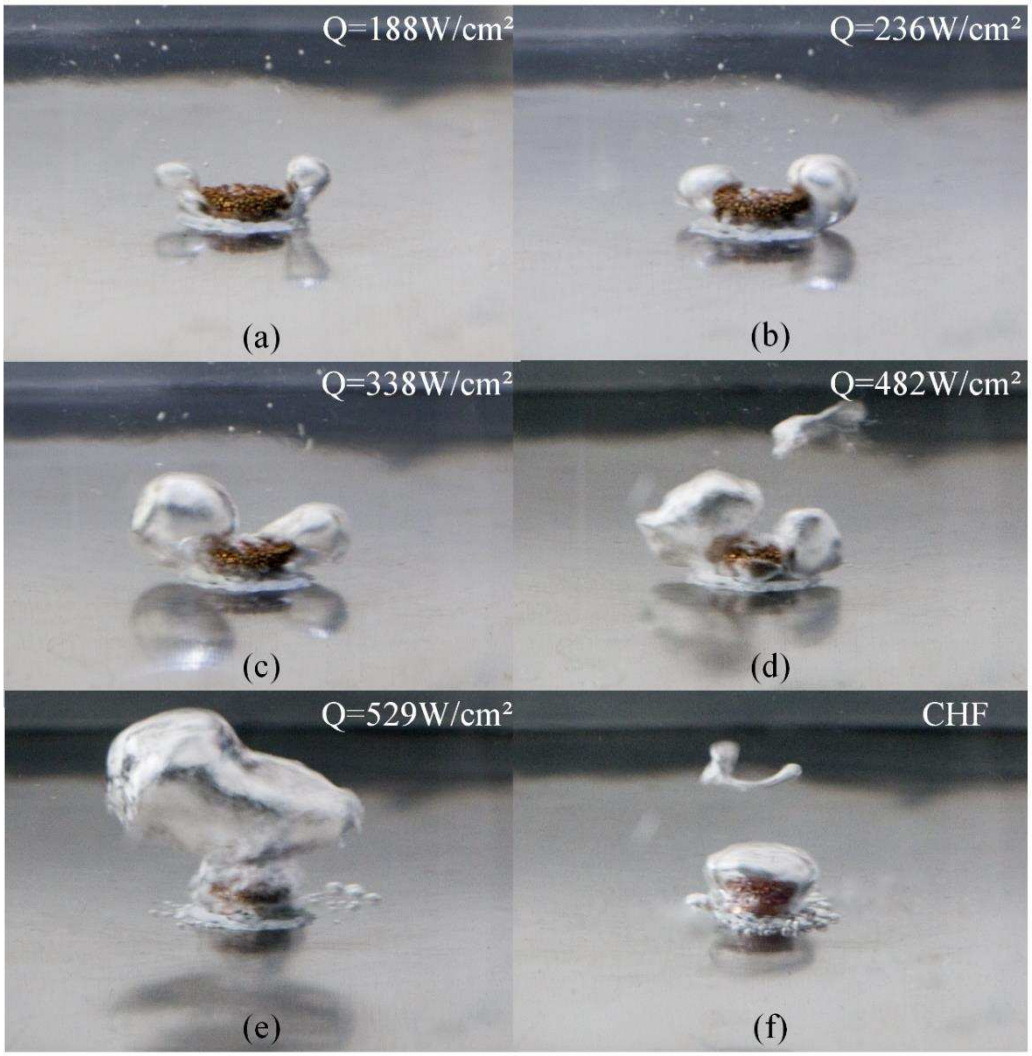

Fig. 5 Liquid/vapor distribution and movement for different heat fluxes (microporous plate thickness: 2 mm, diameter: 8 mm)

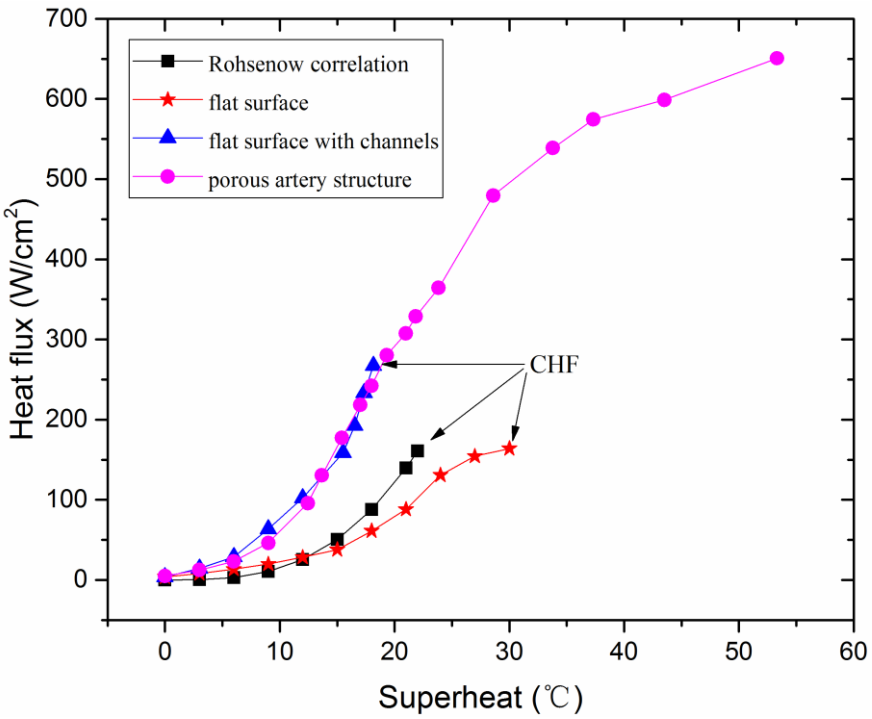

Fig. 6 Superheat dependence of heat flux for pool boiling with different cases (microporous plate thickness: 4 mm, diameter: 8 mm; channel width and depth: 0.8 and 1.5 mm)

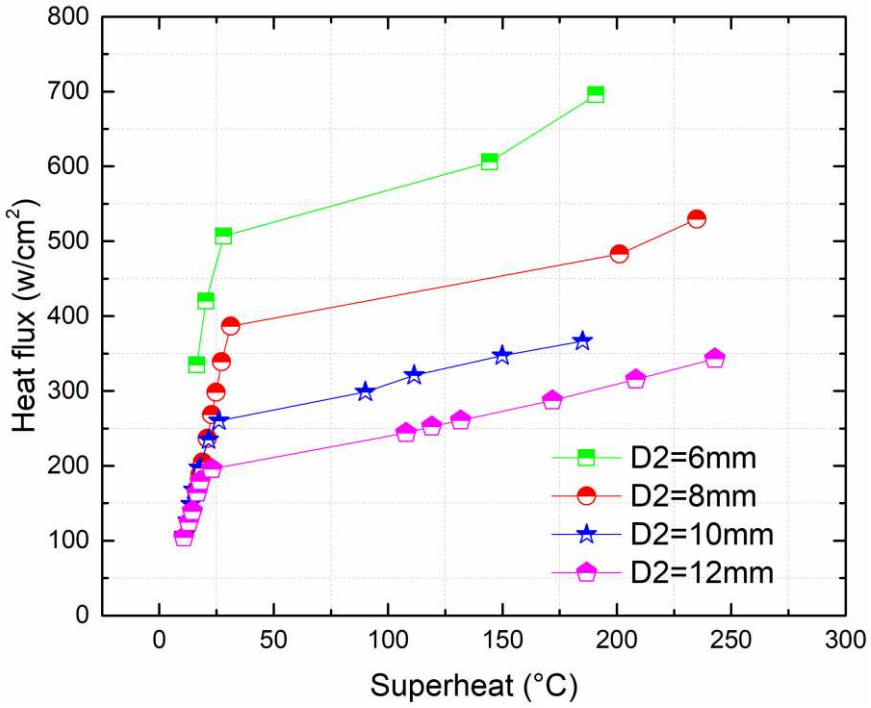

Fig. 7 Effect of the diameter of porous plate on the pool boiling performance (microporous plate thickness: 2 mm, diameter: 6, 8, 10 and 12 mm)

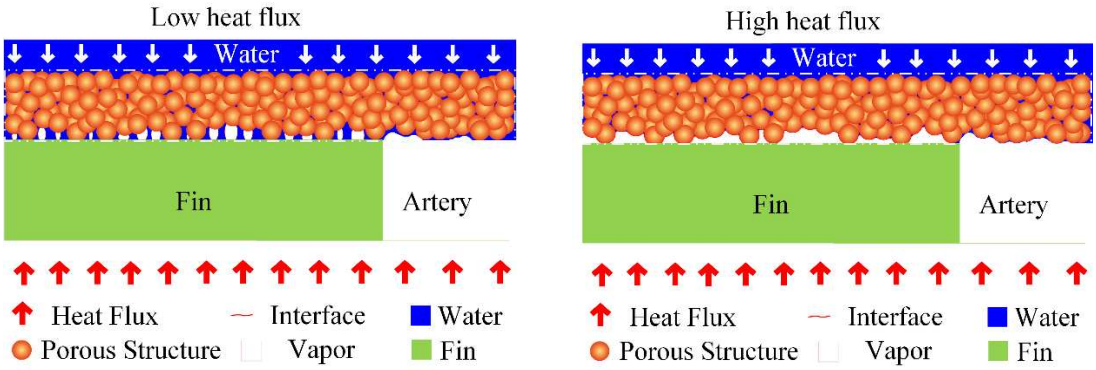

(a) Small and moderate heat fluxes (b) Large heat fluxes

Fig. 8 Schematic of liquid/vapor distribution in the porous structure with different heat fluxes

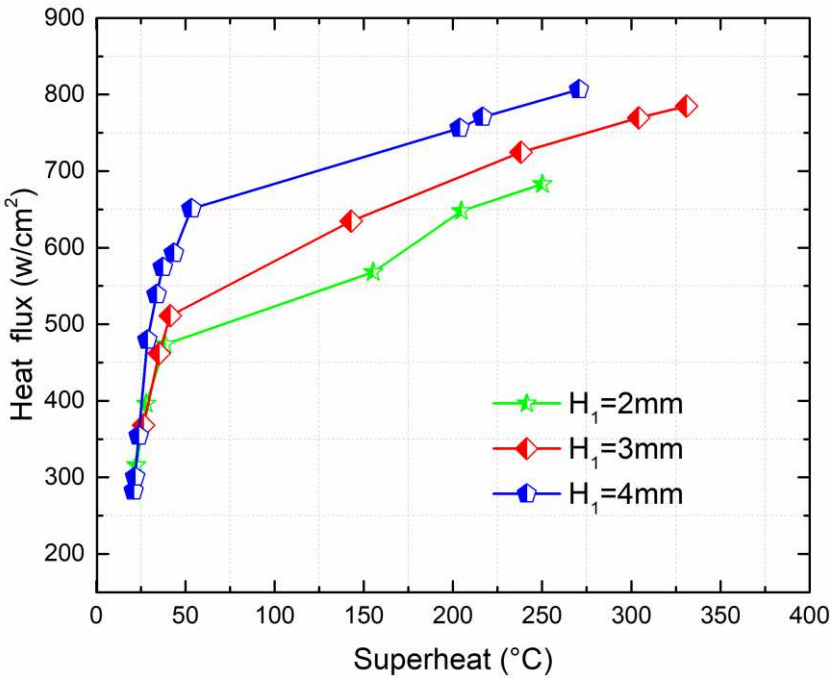

Fig. 9 Effect of the thickness of porous plate on the pool boiling performance (microporous plate diameter: 8 mm, thickness: 2, 3 and 4 mm)

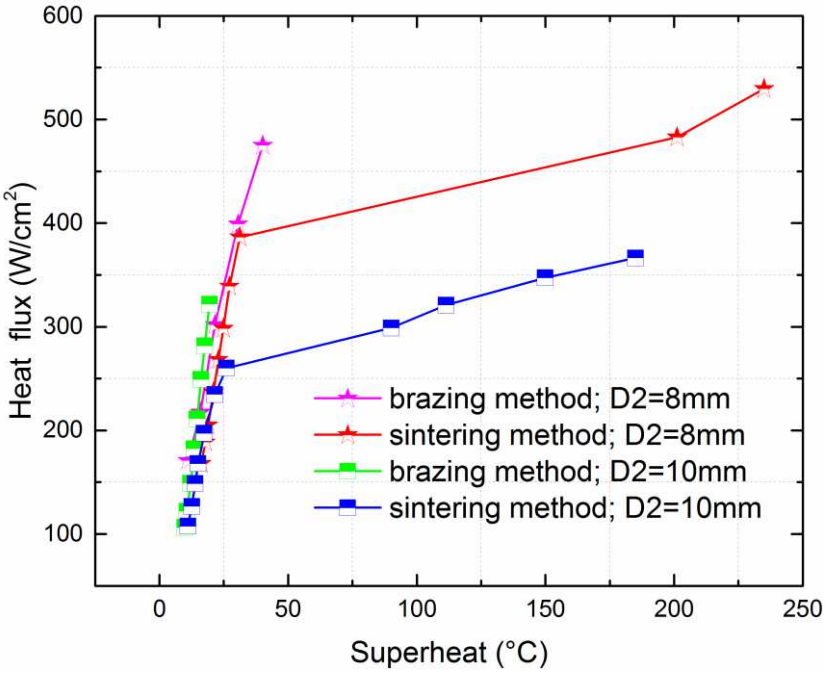

Fig. 10 Effect of connection method on the pool boiling heat transfer performance (microporous plate thickness: 2 mm, diameter: 8 and 10 mm)